Research Article

Development of Hot Equal Channel Angular Processing (ECAP) Consolidation Technique in the Production of Boron Carbide(B4C)-Reinforced Aluminium Chip (AA6061)-Based Composite

Sami Al-Alimi[a], Mohd Amri Lajis[a*], Shazarel Shamsudin[a], Nur Kamilah Yusuf[a], Boon Loong Chan[a], Djamal Hissein Didane[a], Mohammed H. Rady[b], Huda M. Sabbar[c], Munthader S. Msebawi[c]

[a]*Sustainable Manufacturing and Recycling Technology, Advanced Manufacturing and Materials Center (SMART-AMMC), Universiti Tun Hussein Onn Malaysia, 86400 Parit Raja, Batu Pahat, Johor, Malaysia*

[b]*College of Engineering, Wasit University, Kut, Iraq*

[c]*Department of Mechanical and Manufacturing Engineering, Faculty of Engineering, Universiti Putra Malaysia, 43400 Serdang, Selangor, Malaysia*

ABSTRACT. The production of metal matrix composites (MMCs) through recycled materials is a cost-saving process. However, the improvement of the mechanical and physical properties is another challenge to be concerned. In this study, recycled aluminium 6061 (AA6061) chips reinforced with different volumetric fractions of boron carbide (B4C) were produced through hot equal channel angular processing (ECAP). Response surface methodology (RSM) was carried out to investigate the dependent response (compressive strength) with independent parameters such as different volumetric fractions (5-15%) of added contents of B4C and preheating temperature (450 − 550°C). Also, the number of passes were examined to check the effect on the mechanical and physical properties of the developed recycled AA6061/B4C composite. The results show that maximum compressive strength and hardness of recycled AA6061/B4C were 59.2 MPa and 69 HV respectively at 5% of B4C contents. Likewise, the density and number of pores increased, which were confirmed through scanning electron microscope (SEM) and atomic force microscopes (AFM) analysis. However, the number of passes enhanced the mechanical and physical properties of the recycled AA6061/B4C composite. Therefore, the maximum compressive strength and hardness achieved were 158 MPa and 74.95 HV for the 4th pass. Moreover, the physical properties of recycled AA6061/B4C composite become denser of 2.62 g/cm³ at the 1st pass and 2.67 g/cm³ for the 4th pass. Thus, it can be concluded that the B4C volumetric fraction and number of passes have a significant effect on recycled AA6061 chips.

Keywords: Aluminium Chips; Hot ECAP; Severe Plastic Deformation (SPD); Metal Matrix Composites (MMCs); Solid-state Recycling

1. Introduction

Aluminium metal is the most significant abundant metal in the Earth's crust and is the third most abundant element, after oxygen and silicon. It makes up about 8% by weight of the Earth's solid surface. Its engineering specifications such as availability, high strength-to-weight ratio, easy machinability, durability, ductility, and malleability make it a preferred metal for various industrial applications (Ahmad, Lajis, and Yusuf 2017).

Direct recycling method (conversion method) is among many novel techniques to reproduce the scraps into finished products and always preferred because it does not require a smelting process and can recover about 92.2% of the total amount of the material (Tekkaya *et al.* 2009). The main advantages of applying direct recycling method are saving energy, reducing labour costs, and protecting the environment by decreasing pollution and emission level (Ahmad *et al.* 2018), (Yusuf, Lajis, and Ahmad 2019). About 5% of the energy required to recover aluminium metal from needed energy compared to the production of the material from ore sources while the conventional direct recovery process results in 40% metal loss. As such, many authors also concluded that the direct conversion method results in lower operating costs and energy consumption (Al-alimi *et al.* 2020), (Al-Alimi, Lajis, and Shamsudin 2017). Aluminium production from ores consists of seven primary steps. It commences from

---

* Corresponding author: samialalimi@gmail.com

alumina production, primary aluminium production, semi-fabrication, and recycling by remelting for metal productions. The metal production through recycling consists of four main steps, which are semi-fabrication, product manufacture, use phase, and recycling (AZOM 2013). To recover metal and remain its superior material properties, the ECAP technique is proposed to form the recycled metal in either pure or composite form. ECAP is a superior metal consolidation method in SPDs to produce nanometre to submicron materials and has gained great attention in the last few years (Azushima *et al.* 2008), (Gode 2019). The ECAP technique has been widely applied to pure metallic alloys such as aluminium, and the experiments were commonly performed at room temperature (Arab *et al.* 2014). The ECAP was invented in the 1970s for metal-forming process with the highest possible strain rate (Dobatkin, Zrnik, and Mamuzič 2010). B4C is an essential hard ceramic material with excellent properties. It has low density, high abrasion resistance, high tensile strength, high melting point level, high impact resistance, low coefficient of thermal expansion, and stable chemical stability. These properties make it an excellent material for reinforcing composites (Kačmarčik, Pepelnjak, and Plančak 2012).

Haghighi *et al.* (2012) commented that the ECAP was a better processing method of all SPDs and discussed the possibility of MMC production through the metal-forming consolidation technology. Nevertheless, the study was lacking in terms of the reinforced material and parametric variables investigated to produce reliable MMCs. Mani and Paydar (2010) presented the applications of SPD consolidation of machined chips of hot forward extrusion and ECAP. The findings show that the ultimate tensile strength and ductility are 148 MPa and 21.6%, respectively, which were obtained from Al reinforced with 10% SiC. The findings for Forward Extrusion (FE) samples are 136 MPa and 16.6%, respectively, which shows an increase in the strength and ductility for the MMC composites formed by FE-ECAP technique. Derakhshandeh-Haghighi *et al.* (2012) consolidated 99.29% and 98.25% of aluminium powders with 5% nano-Al₂O₃ at 200°C by ECAP. The results show better-enhanced measurements of material hardness, microstructure bonds, and wear resistance for the material made with ECAP process compared to that from the hot extrusion process. Lokesh and Mallik (2016) fabricated samples of 10 mm diameter and 80 mm length that were machined from cast hybrid composite for ECAP process. The friction was reduced by polishing the samples using SiC abrasive papers, and the samples were annealed at 400°C for 4 h to homogenise the microstructure. All samples were subjected to a series of ECAP process using 10 mm diameter tool with two channels intersecting at the inner and outer angles of $\phi = 120°$ and $\psi = 12°$ respectively. Harichandran and Selvakumar (2015b) studied the effect of adding micro-nano-B4C particles by using the technique of casting process. They found that material incorporated with 6% nanoparticles exhibited better mechanical properties such as higher tensile strength, ductility, and impact resistance compared to micro-B4C-reinforced particles.

Researchers have investigated the effects of adding ceramic particles on the light metal aluminium composites. However, there are still many aspects for the researchers to discover in direct chip recycling by hot ECAP process, such as the effect of prepared scraps quality (influenced by the machining parameters), cleaning, drying and composite mixing. Also, the ECAP process factor such as pressing speed, pressing force, and inner and outer angles. Therefore, no work has been done to investigate the material properties of recycled aluminium-based composite reinforced with B4C using hot ECAP process.

This research aimed to develop aluminium alloy (AA6061) chips-based composite reinforced with 7±3 μm of B4C powder. The volume fractions of B4C samples were 5%, 10%, and 15%. The mechanical, physical, and microscopic properties were investigated by using the reinforcement of B4C. MMCs are resulting in promising applications in industrial manufacturing of defence and automotive applications. So, to investigate the effects of reinforcement AA6061 aluminium as an area to be studied and introduced with a new approach of solid-state recycling by using hot ECAP with lower energy consumed where the current trends in MMC production have a high potential in the automobile engineering industries (valve train, piston rod, covers, piston pin and piston, cylinder head, main crankshaft bearing, engine block, and cylinder blocks).
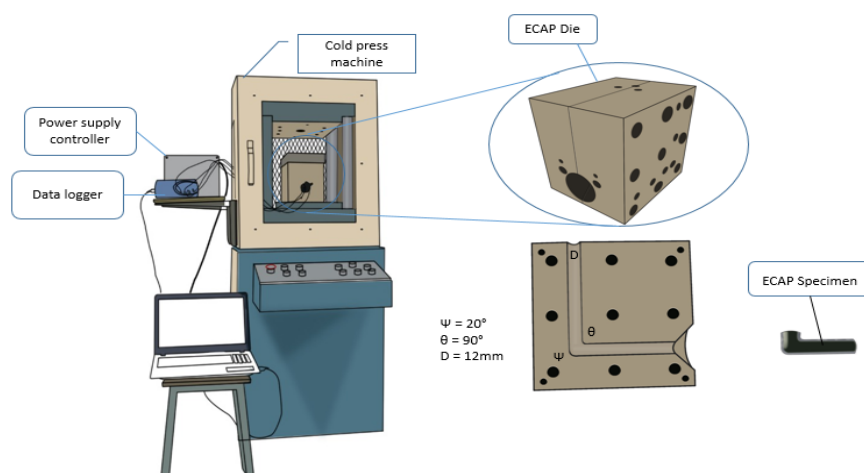

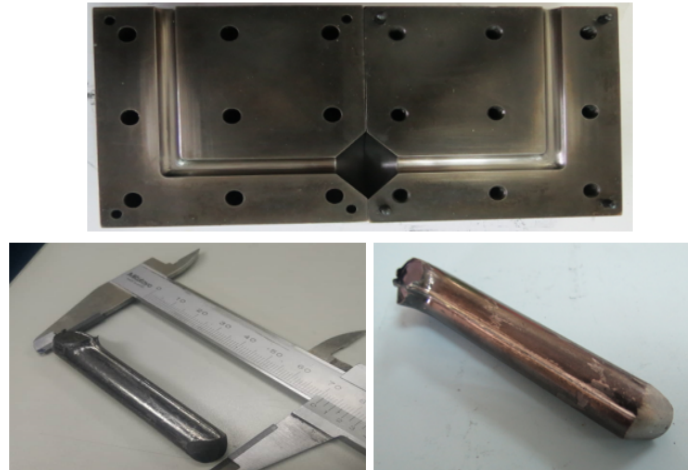**Fig 1.** Hot ECAP die and related accessories

Fig 2. Hot ECAP die products of recycled Al/B$_4$C-based composite.

2. Materials and Methods

Aluminium alloy AA6061 chips of less than 4 mm length and B4C powder with an average size of 7±3 µm were utilised as matrix and reinforcing materials, respectively. The effect of different volumes of B4C added to AA6061 chip-based composite with a density of 2.7 g/cm^3 and elasticity of 70 GPa was studied thoroughly. The AA6061 contains magnesium, silicon, copper, iron, and zinc as major alloying elements (Poovazhagan *et al.* 2013). The volume fraction of the B4C powder was varied to 5%, 10%, and 15%. The hot ECAP die in this study was specifically designed to fabricate the chip-based MMCs effectively. The experimental design of the research work consists of two stages. During the first stage (screening), the experiments were performed according to the full factorial design. Two main parameters were carefully studied, which were the volumetric percentage of B4C (5%, 10%, and 15%) and processing temperature (450, 500, and 550°C). For the second stage, the experimental runs were designed according to the face-centered central composite design (CCD). As the name implies, the star points in face-centered CCD design were located at the face of the cube portion, corresponding to an α-value of 1 while the centre points were points with all levels set to 0. Two replicates of experiments were carried out at each factorial run, and a single replicate run was carried out at axial points that led to 12 runs in total. At the centre point, 3 replicates were selected, and as a result, 15 runs in total were involved throughout the experiments. The three centre points in the design were initially used to test the curvature effect of the model; if significant, the model would be further analysed through quadratic form by RSM design. The Minitab 18 software simplified the analysis of variance (ANOVA) calculation and empirical model development. The statistical analysis obtained the optimum value of the compressive strength (analysed response) of hot ECAPed specimens through a combination of factors which were calculated simultaneously by the Minitab 18 (Nemati-chari *et al.* 2015).

A new ECAP system was designed for this research, and it commenced from pressing all sides of the specimen through four different passes as depicted in the schematic diagram (Figure 1 and 2). Figure 1 shows the pressing of the side A of the specimen and the rest shows the pressing of remaining sides of the specimen. The system comprises hydraulic cold press machine, hot ECAP die, and related accessories as shown in Figure 2. The maximum capacity of the mean press machine was 50 tonnes with the bottom single-cylinder movement type to avoid damage on the plunger and die, the pressing force was set between 12 and 15 tonnes, and the vertical pressing velocity applied was 7 mm/min. The ECAP die consists of two parts with a channel of 12 × 12 mm and four blind holes were embedded for attaching cartridge type of heaters. On top of that, the heat generated was measured by a K-type thermocouple with a 3 mm diameter. Details of ECAP die configuration with an inner angle (ϕ) = 90° and outer angle (Ψ) = 20° are shown in Figure 3.
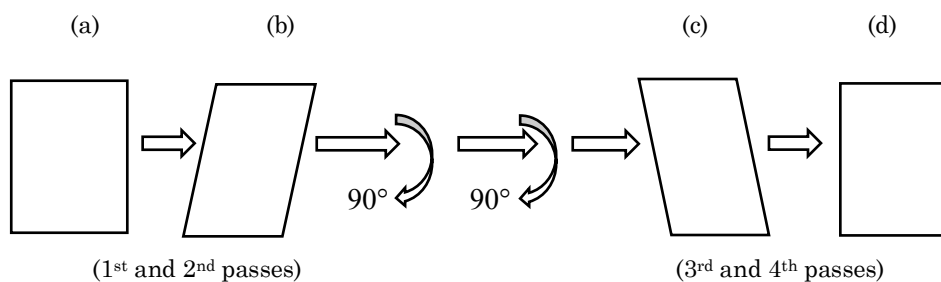

Fig 3. Streamlined patterns of different ECAP passes for a to d routes (Fang et al. 2006).

The hot ECAP was used to produce billets with enhanced strain and superior mechanical properties. The effective theoretical strain, according to the die geometry, is given by Equations (1) and (2). The ECAP route affects the forming process of light metals, mechanical properties of MMCs, microstructure formation, and accumulated strain (Djavanroodi and Ebrahimi 2010). The strain for a single pass could be calculated by Iwahashi's equation (Eq 1).

$$\epsilon = \frac{1}{\sqrt{3}}\left(2\left(cot\,\frac{\Phi+\Psi}{2}\right) + \frac{1}{\sqrt{3}}\left(\Psi\,csc\,\frac{\Phi+\Psi}{2}\right)\right) \qquad (1)$$

The efficient strain of multiple passes is calculated as follows (Djavanroodi and Ebrahimi 2010).

$$\epsilon_{eq} = N\,\epsilon \qquad (2)$$

where ϵ = the strain for a single pass, ϵ_{eq} = the strain for multiple passes, Φ = inner angle, Ψ = outer angle, and N = no. of passes. The number of passes in the ECAP process is the most influential factor that has been considered by researchers according to the calculated total strain to achieve the desired strain distribution (Djavanroodi *et al.* 2012). Equation 2 explains the equivalent effects of the average developed strain on the specimens within frictionless conditions. However, in reality, the surface between the die wall and the specimen is unavoidable. The hydraulic pressing machine induced the imposed strain, and the required pressure for pressing, P, of the sample is presented in Equation 3 (Djavanroodi and Ebrahimi 2010).

$$P = \tau_0(1+m) = \left(2\left(cot\,\frac{\Phi+\Psi}{2}\right) + \Psi\right)\left(4\,m\tau_0\,\frac{l_i+l_0}{a}\right) \qquad (3)$$

Where τ_0, m, $l_i + l_0$, and a are the shear strength, friction coefficient, instant length of the sample of both entry and exit channel, respectively.

The temperature of hot ECAP die was set to 300°C by five embedded K-type thermocouples on the die, and four heater rods were used to generate and evenly distribute the heat throughout the die. Furthermore, the TC-08 data logger with K-type thermocouples and heater rods were interconnected to measure the temperature distribution and provide feedback to the controller for regulating the heat into the die. The die was encapsulated by a customised casing equipped with a unique insulation material to retain the heat. The extruded samples were then measured in terms of their compressive strength (ASTM E9 – 09) and hardness (ASTM E92 - 82). The compressive test was carried out by the universal testing machine (UTM Instron type), and the hardness test was carried out by the Vickers hardness tester. Performing The samples are characterized by using AFM (MODEL: XE-100) and SEM (model no: JEOL JSM-6380LA MP-19500014) to investigate the reinforced particles distribution, chip boundaries and measuring the grains size of the samples.

The DOE Pareto chart shows the magnitude and significant effects of any performed investigation. Figure 4 shows B, A, BA, and AA bars. The investigated model can be considered statistically significant if these bars cross the reference line at 0.05 level. Moreover, the standardised effect of the model was analysed through a t-

statistic test for testing the null hypothesis. However, positive effects increase responses when the setting changes from low values of the factor to high values. Negative value settings decrease the response values. Nevertheless, the effect from 0 on the x-axis is more significant, and the results starting from 0 are statistically more significant. Also, The statistical significance of the distance of all points depends on the point level denoted by α. Meanwhile, the response of the investigated model can be found through expected probability and other parameters of the model, as shown in Figure 4. The normal probability plot determines the direction, magnitude, and significance of effects. Also, the plot confirms that the B4C volume fraction (B) and preheating temperature (A) have a standardised effect when the process was varied from lower to a higher level.

According to the regression model and RSM analysis of variance (ANOVA), the quadratic model suggests for the explanation of the effects of heating temperature and B4C volume fraction on the investigated model to check the compressive strength of the composite material. Furthermore, the ANOVA indicates that the processing parameters (temperature [A], volume fraction [B], temperature*volume fraction [AB], and temperature*temperature [AA]) were significant. The overall model quality could be evaluated based on the results of R^2, adj. R^2, pred. R^2, and adequate precision values.
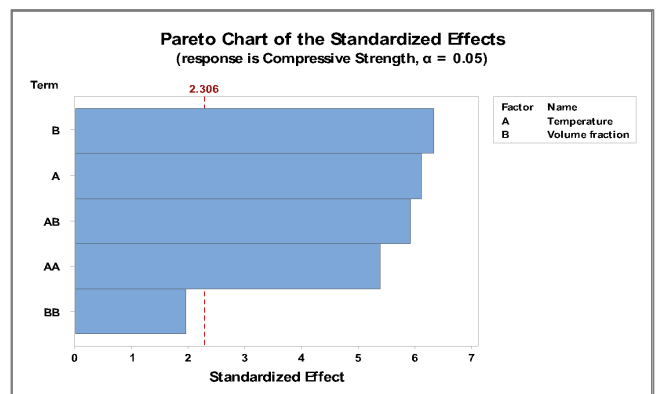

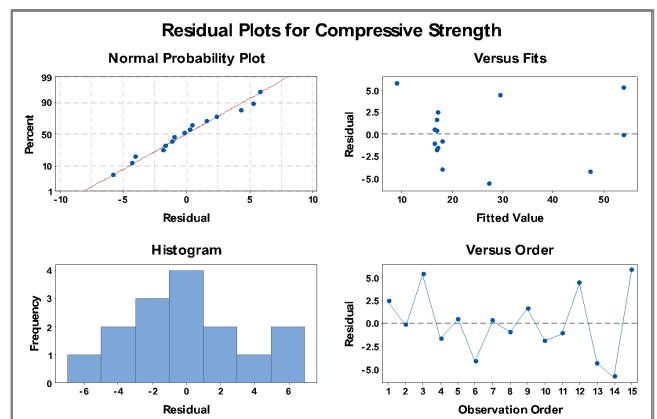**Fig 4.** Pareto chart of the compressive strength response

Fig 5. Response analysis of RSM.

Table 1
Analysis of variances for compressive strength.

Source	DF	Adj SS	Adj MS	F Value	p Value
Model	6	3009.96	501.660	24.17	0.000
Blocks	1	120.34	120.340	5.80	0.043
Linear	2	1615.93	807.963	38.93	0.000
Temperature	1	781.81	781.810	37.67	0.000
Volume fraction	1	834.12	834.117	40.19	0.000
Square	2	606.25	303.126	14.61	0.002
Temperature*Temperature	1	606.19	606.186	29.21	0.001
Volume fraction*Volume fraction	1	79.35	79.353	3.82	0.086
2-Way Interaction	1	729.24	729.238	35.14	0.000
Temperature*Volume fraction	1	729.24	729.238	35.14	0.000
Error	8	166.01	20.752		
Lack-of-Fit	2	130.60	65.298	11.06	0.010
Pure Error	6	35.42	5.903		
Total	14	3175.98			

Table 2
Table of model summary.

S	R^2	Adj. R^2	Pred. R^2
4.55541	94.77%	90.85%	73.24%

Table 3
Regression coefficients of the compressive strength.

Term	Coef.	SE Coef.	t Value	p value	VIF
Constant	20.22	2.31	8.74	0.000	
Blocks					
1	−3.31	1.38	−2.41	0.043	1.07
Temperature	8.84	1.44	6.14	0.000	1.00
Volume fraction	−9.13	1.44	−6.34	0.000	1.00
Temperature*Temperature	14.87	2.75	5.40	0.001	1.22
Volume fraction*Volume fraction	−5.38	2.75	−1.96	0.086	1.22
Temperature*Volume fraction	−9.55	1.61	−5.93	0.000	1.00

$$\begin{aligned}
Compressive\ Strength = {} & 1224 - 5.39\ Temperature + 21.57\ Volume\ fraction \\
& + 0.00595\ Temperature * Temperature \\
& - 0.215\ Volume\ fraction * Volume\ fraction \\
& - 0.03819\ Temperature * Volume\ fraction
\end{aligned} \tag{4}$$

The quadratic model obtained mathematical modelling with a strong determination of R^2 = 94.77%, which is a good regression model fitted to the research observations. The adj. R^2 and pred. R^2 values were 90.85% and 73.24%, respectively. A good agreement between the adj. R^2 and pred. R^2 prevents the overfitting of the mathematical model. Table 1 shows the results of compressive strength through ANOVA.

The P-value was introduced to test the static effectiveness of the proposed model with the factors. The important effects of P-value to the processed parameters which must be lower than 0.05. if greater than 0.05. It shows no important effects on the responses as presented in Table 3.

The data was analysed to obtain the appropriate level of the studied factors which causes enhancement of compressive strength properties and the regression equation. From the regression coefficients and analysis of variance of the compressive strength, as shown in Tables 4 and 6, the obtained p values of the preheating temperature (0.000) and B_4C volume fraction (0.001)

confirm that the data are significant. The quadratic equation, in which R^2 = 94.77% and adj. R^2 = 90.85%, confirms coefficient of P regression value which is 0 < α. The functional quadratic regression is curvature and the tested variable of compressive strength. However, the axil added design is a must to apply and the mathematical model is expressed in Equation 4.

The mean effects of presented parameters on the compressive strength of recycled composite material were investigated. The experimental findings identify the interactions as their related changes in the design of the reinforced volume fraction of B4C particles and preheating processing temperature. Increasing the B4C volume fraction and processing temperature resulted in resulted compressive strength up to 5% vol. B4C and 550°C temperature. At the same time, the minimum plotted values of 15% vol. B4C and 450°C temperature resulted in decreased compressive strength. Moreover, the quadratic model has been proposed and shows the significance of analysed factors.
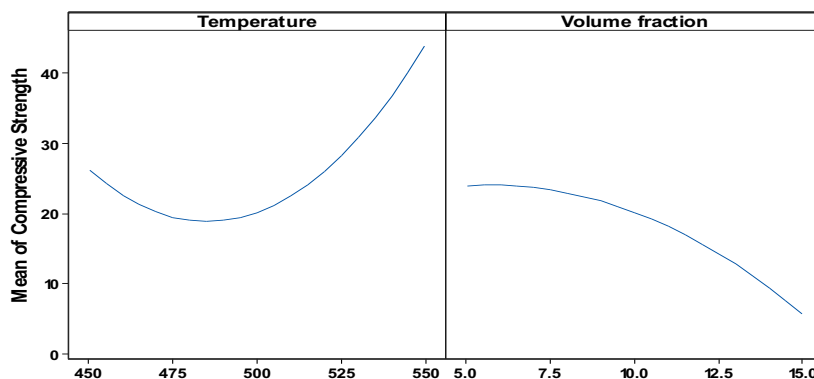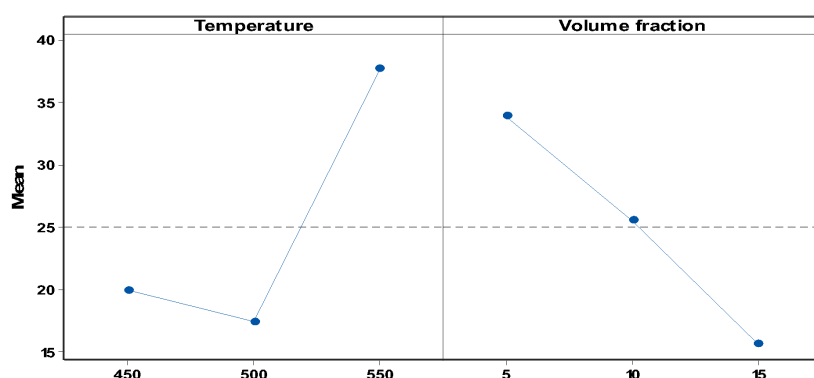
Fig 6. Mean effects plot for compressive strength.

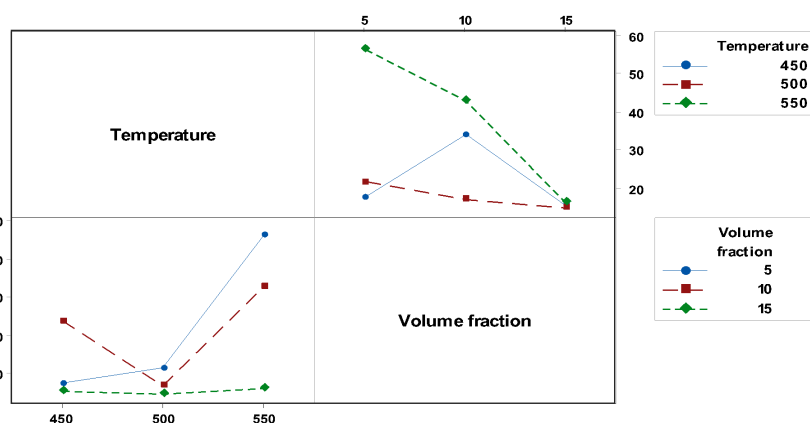**Fig 7.** Mean effects plot for compressive strength.

Fig 8. Interaction plot of compressive strength.

Maximising the findings approach with an axial design was performed for each control factor of the model. The RSM in Figures 6 and 7 present the experimental compressive strength values, which increased with increasing the preheating temperature to 550°C and at 5% vol. B4C. Therefore, the optimum compressive strength was obtained at 5% B4C volume fraction ceramic particles and 550°C preheating temperature. A volume fraction exceeding 5% caused a decrease in the compressive strength of recycled MMC. The graphical representation of the hot ECAP preheating temperature and B4C contents is shown in Figure 8. The temperature increment within the B4C particles enhanced the mechanical and physical properties of the recycled MMCs. Figure 10 shows the 3D surface plot for the compressive strength and the optimum values recorded by more design of experiment (DOE) analysis. Through observing previously, the most influential factors were B4C contents and preheating temperature, an additional agreement induced by the severe plastic strain refinement.
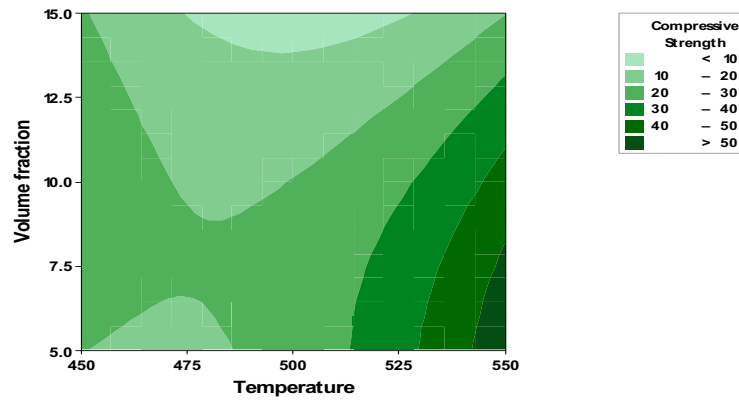
Fig 9. 2D compressive strength surface response.
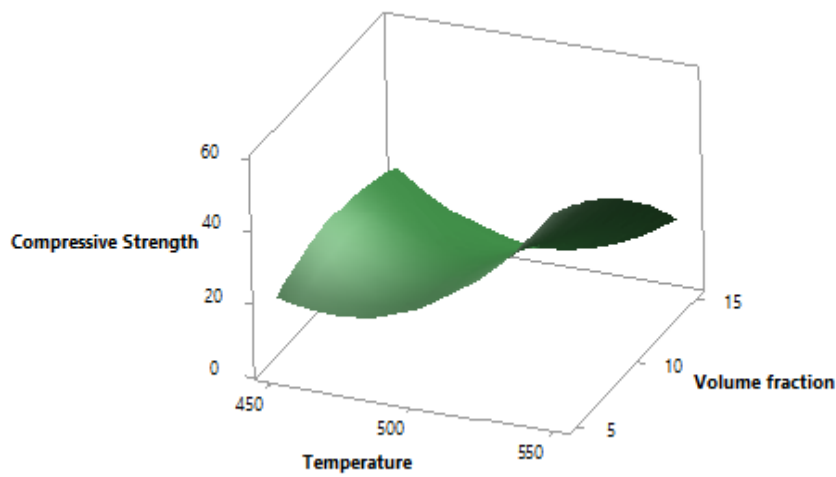
Fig 10. 3D surface plot of compressive strength, B_4C volume fraction, and temperature.
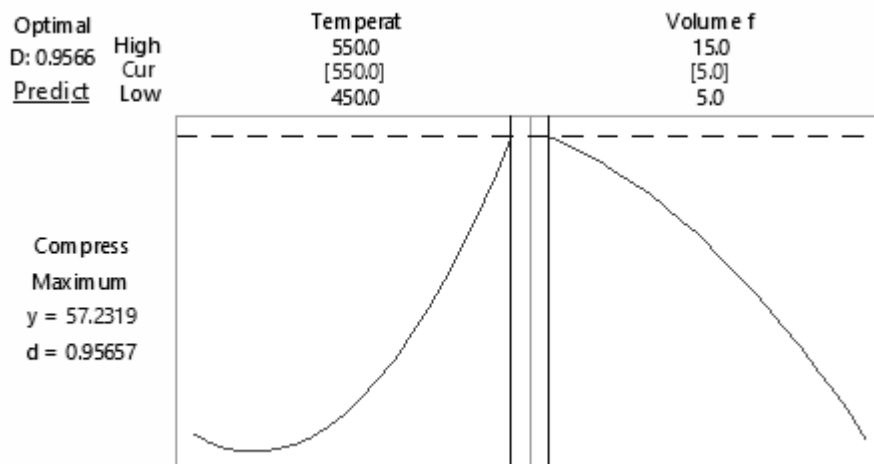
Fig 11. Responses optimiser plot

The responses optimiser was identified as the combined relations of the inputted variables that propose a set of responses. Minitab18 software calculated the RSM optimal solutions and plotted the optimisation graph. The interactive plot could let to have experimental inputted variables presented after the model is fitted. The recycled

MMCs under different volume fractions of B4C and preheating temperature, and the responses are maximised at 5% B4C and 550°C preheating temperature. So for selected maximising the response as the higher is better and for minimising the responses, the smaller is better as shown in Figure 11.

3. Results and Discussions

3.1 Compressive strength

Table 4 shows the compressive strength of the composite with different volume fractions of B4C processed by hot ECAP at 450°C, 500°C, and 550°C preheating temperatures for 3 h. The findings prove that with the increasing volume fraction of B4C, the compressive strength increased significantly until it reaches the optimum value of 59.2 MPa at 5% B4C. Further increases of B4C resulted in a decrease in compressive strength at 10% B4C and 15% B4C. The consolidation of the materials was achieved in which higher mechanical strength was obtained at 5% B4C. The study confirmed that the B4C particles could significantly enhance the aluminium chips. The highest compressive strength of 59.2 MPa was obtained at 550°C and 5% B4C, and the lowest value of 13.88 MPa was obtained at 450°C and 15% B4C due to the continuity of the other particles to the composites samples. This is mainly because the movement and dislocation became hard to occur due to the shortened distance between the particles if B4C volume was further increased. In this situation, pile ups occurred, and the composite samples became less dense, which led to lower compressive values. The error values between RSM and experiment is 1.97 which is very close to each other. Higher preheating temperature results in a higher compressive strength due to the high metallic bonding of consolidated chips. Therefore, it can be seen that the overall maximum compressive strength is obtained at the 5% B4C volume fraction of the highest compressive strength and at the preheating temperature of 550°C.

3.2. Effects of B4C particles on hardness

The hardness investigations were conducted to test the material resistance when a particular force is applied (Ramnath *et al.* 2014). The hardness test on the composites will reveal the composite's resistance to the local plastic deformation. Each sample was indented at five different spots, and the average value was calculated to examine the sample's hardness. Table 5 shows the results of hardness and density for the added composite with different B4C contents. The hardness is positively correlated to the B4C volume fraction weight that increased up to 10%. The composite made with 10% B4C at 550°C had superior consolidation characteristics. Furthermore, the hardness of the composites decreased at 15% B4C due to the availability of pores and particle agglomeration. Further increase in the B4C volume fraction yielded too large pores of the materials which increased the voids in sizes and numbers with the formation of stress concentrations.

3.3. Effects of B4C particles on density

The samples were weighed in air and distilled water separately following Archimedes's principles. The theoretical and experimental average density of the recycled composites were obtained for each sample produced using different volume fractions of B4C. The Archimedes theory was employed to measure the density of samples, and the calculated densities were obtained by using the following formula.

$$\frac{1}{\rho_c} = \frac{w_f}{\rho_f} + \frac{w_m}{\rho_m} \tag{5}$$

Where ρ is density, w is volume fraction, while m, f, and c are related to the composites and reinforcement. From the results, the overall densities decreased with the increase of volume fraction of B4C particles. This is due to the lower density of B4C particles (2.52 g/cm^3), which is less than the pure AA6061 aluminium density. Therefore, the MMC density is slightly lower than the pure aluminium because of the differences in both values (Alizadeh and Aliabadi 2011). By increasing the amount of B4C contents, the pores increased (Ramu and Bauri 2009). The percentage of porosity was obtained from the difference between the theoretical and measured densities.

3.4. Energy Dispersive Spectroscopy (EDS)

The energy dispersive spectroscopy (EDS) analysis involves a crystal that absorbs the directed energy of the X-rays ionisation method. In this research, the composites of 5% vol. Al-B$_4$C, 10% vol. Al-B$_4$C and 15% vol. Al-B$_4$C were analysed with EDS over the representative regions of presented samples (Djavanroodi and Ebrahimi 2010). Also, the EDS results shown in Figure 12 indicate the composite contamination of the ECAPed samples from the forming process, and these effects were dispersed accordingly on the composite reinforcement distribution. The test analysis confirms that B$_4$C particles through hot ECAP reflection form is investable. The aluminium chips and B$_4$C particles were fully consolidated, and the lower oxygen content results in better composite fabrication protection.

3.5. X-ray diffraction (XRD)

The X-ray diffraction (XRD) patterns of AA6061/B$_4$C recycled ECAPed composite specimens at different B$_4$C volume fractions are illustrated in Figure 13. The different temperatures ranging from 450 to 550°C on recycled samples resulted in good bonding with the material matrix. The XRD pattern of recycled AA6061/B$_4$C MMCs shows the presence of B$_4$C, Al, and no other elements were present as an important quaintly of the matrix reactions (Rebhi *et al.* 2009). The findings indicate that the B$_4$C contents reacted with AA6061 to produce other compounds. However, the process shows it is thermodynamically involved synthesising temperature stability, and the reactions of the ECAPed samples were desirable in an intermetallic compound that would affect the mechanical and physical properties of the material.

Table 4
Compressive strength with different B_4C contents processed by hot ECAP.

Sample notation	Std. order	Run order	V. F (B_4C) (%)	Temperature (°C)	Compressive Strength (MPa)
S_1	1	4	5	450	15.5
S_2	2	2	5	550	53.7
S_3	3	8	15	450	17
S_4	4	11	15	550	15.4
S_5	5	1	5	450	19.5
S_6	6	3	5	550	59.2
S_7	7	6	15	450	13.88
S_8	8	5	15	550	17
S_9	9	7	10	500	17.2
S_{10}	10	10	10	500	15.03
S_{11}	11	9	10	500	18.5
S_{12}	12	12	10	450	33.90
S_{13}	13	13	10	550	42.90
S_{14}	14	14	5	500	21.51
S_{15}	15	15	15	500	14.80

Table 5
Calculated and measured densities and hardness results.

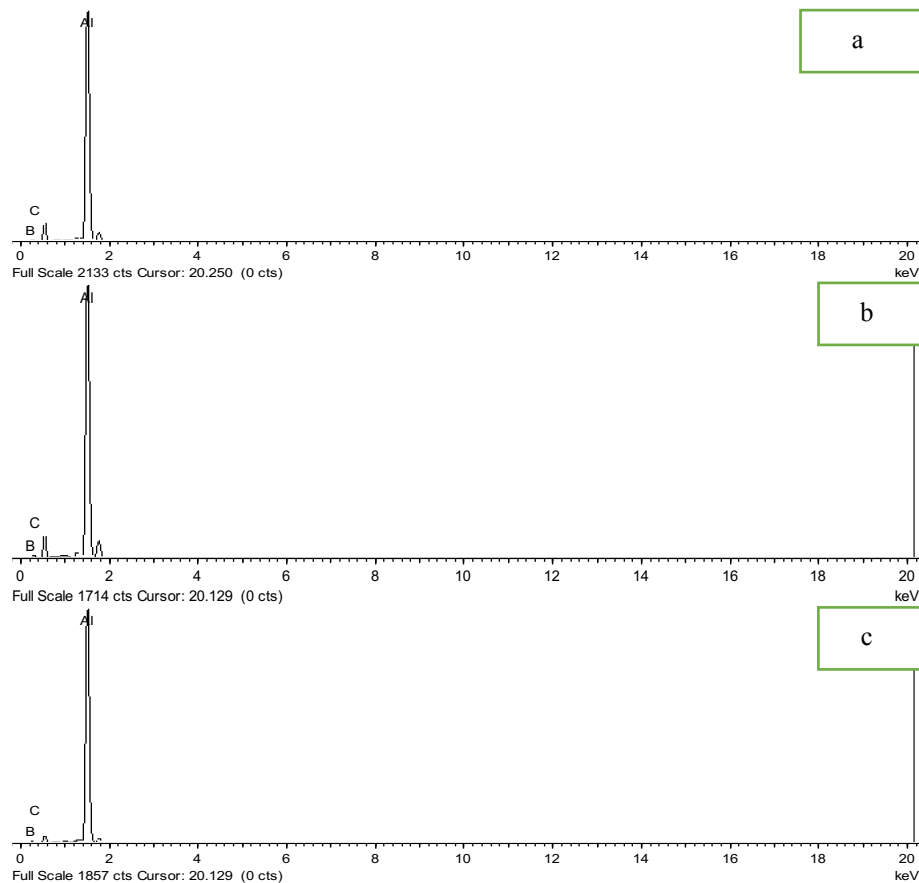| Materials	Theoretical Density (g/cm³)	Experimental Density (g/cm³)	Pores %	Mean Hardness (HV)
B_4C	2.52	-		-
AA6061	2.7	-		-
Al-5 vol.% B_4C	2.69	2.47	0.22	44.23
Al-10 vol.% B_4C	2.68	2.44	0.24	68.85
Al-15 vol.% B_4C	2.67	2.42	0.25	53.92

Fig 12. EDS analysis of recycled Al-B_4C composites, (a) Al-5 vol. % B_4C, (b) Al-10 vol. % B_4C, (c) Al-15 vol. % B_4C
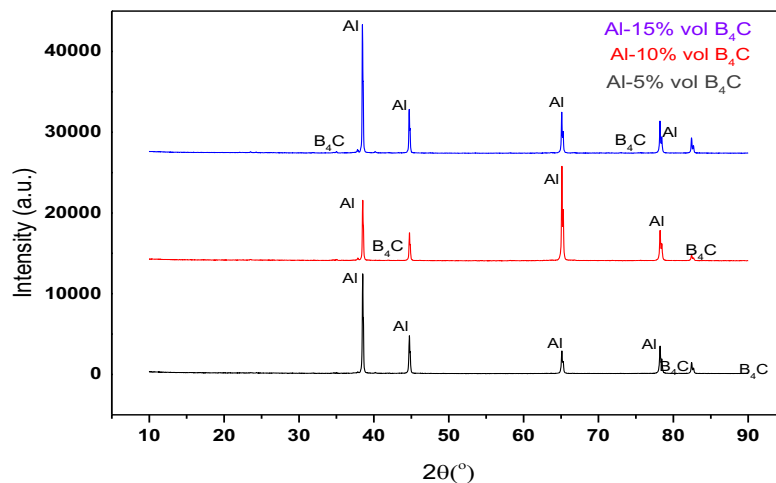
Fig 13. X-ray diffraction of recycled Al-B$_4$C composites

Table 6
AFM mean grain size and surface roughness.

Samples	Mean grain size (µm)	Ra (nm)	Rq (nm)
5% vol. B$_4$C/Al	0.25	27.65	38.68
10% vol. B$_4$C/Al	0.27	46.62	65.75
15% vol. B$_4$C/Al	0.28	100.26	125.50

3.6. SEM micrographs

Figure 14 shows the SEM images of the recycled MMC with different volumetric percentages of B$_4$C. The contents of B$_4$C were confirmed through SEM analysis. Moreover, few cracks were also observed on the surface of the recycled MMC specimens. The SEM results demonstrate a uniform distribution of the 5% vol. B$_4$C contents without bores and indicate well bonded MMCs composites structures, which was achieved by hot ECAP process. Figure 14b shows the morphology/image of the composite under the ECAP for the 10% vol. B$_4$C and 550°C. Regarding the sample's agglomeration certain pores and cracks could be observed closer to the reinforcement B$_4$C particles in the relations with Figure 14b there were micro-pores and cracks which notified beside the region of the intermetallic phases at lower reinforced particles. Figure 14c shows the observation of pores and cracks for 15% volume fraction, which are closer to the interface zones between the matrix and B$_4$C particles. The 5% vol. B$_4$C and 550°C gave the best results. Indeed, the higher volume fraction caused cracks that led to MMC failure. However, agglomerations could be the most with 15% vol. B$_4$C samples reveal to the presence of detected macro-pores of the MMCs composites.

3.7. AFM pit morphology

AFM is the standard microscopy method for investigating and measuring the thin film surface morphologies of the surface roughness or micro shape of nanoparticles. The AFM is a method for testing conductive materials by investigating the surface topography from microscale to the nanoscale of prepared samples (Luce n.d.). However, thin films exhibit polycrystalline structures and grain measurements which are significant to be recommended for the film's technology. Also, the shapes are the main factor influences on grains radius, length, and so on. Thus, the sharp tip yields to obtain higher accuracy (Karoutsos 2014). AFM is presented to show the material's agglomeration of composites. The results are shown in 3D images of 5% vol. B$_4$C/Al, 10% vol. B$_4$C/Al, and 15% vol. B$_4$C/Al recycled composites at 550°C preheating temperature. The microstructure was altered during the ECAP process depending on the addition of B$_4$C particles to the aluminium chips. The grains were less organised when the volume fraction of particles were distributed, also the appearance of the surface is significantly consolidated after the ECAP forming process. All of the obtained grains, polycrystalline, and structure appear to be dependable on the material's film thickness, and the lateral effective grain distributions are presented in Table 6 and Figure 15. The film thickness of all samples decreased from 0.25 µm, 0.27 µm, and 0.28 µm for 5% vol. B$_4$C/Al, 10% vol. B$_4$C/Al, and 15% vol. B$_4$C/Al, respectively. The most presented lateral decreased scales in the film thickness are 0.25 µm to 0.27 µm. The root means square were 38.681, 65.75, and 125.50 nm for 5% vol. B$_4$C/Al, 10% vol. B$_4$C/Al, and 15% vol. B$_4$C/Al respectively. It is confirmed that the grain size enlargement and film thickness increases of the investigated samples are

related to the increases in the time spent and its growth. Borblik *et al.* (2016) proposed that the decreases in the film thickness result in decreases of all scales characteristics of the material surface relief. Luce *et al.* (Luce n.d.) reported that AFM could be used to analyse different sizes and types of images surface topography with easy sample preparation that is started from the nano- or microscale of the magnetic thin films.
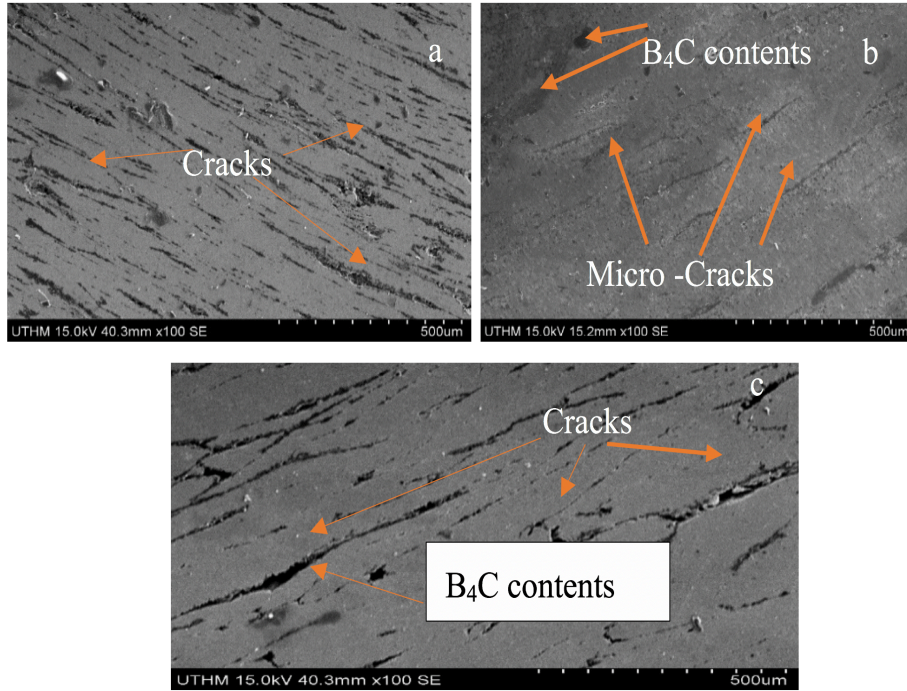

Fig 14. SEM micrographs of (a) (a) Al/5% vol. B_4C, (b) Al/10% vol. B_4C and (c) Al/15% vol. B_4C,.

5% vol. B_4C/Al

$g = 0.25$ μm, Ra = 27.65 nm, Rq = 38.68 nm

10% vol. B_4C/Al

$g = 0.27$ μm, Ra = 46.62 nm, Rq = 65.75 nm

15% vol. B_4C/Al

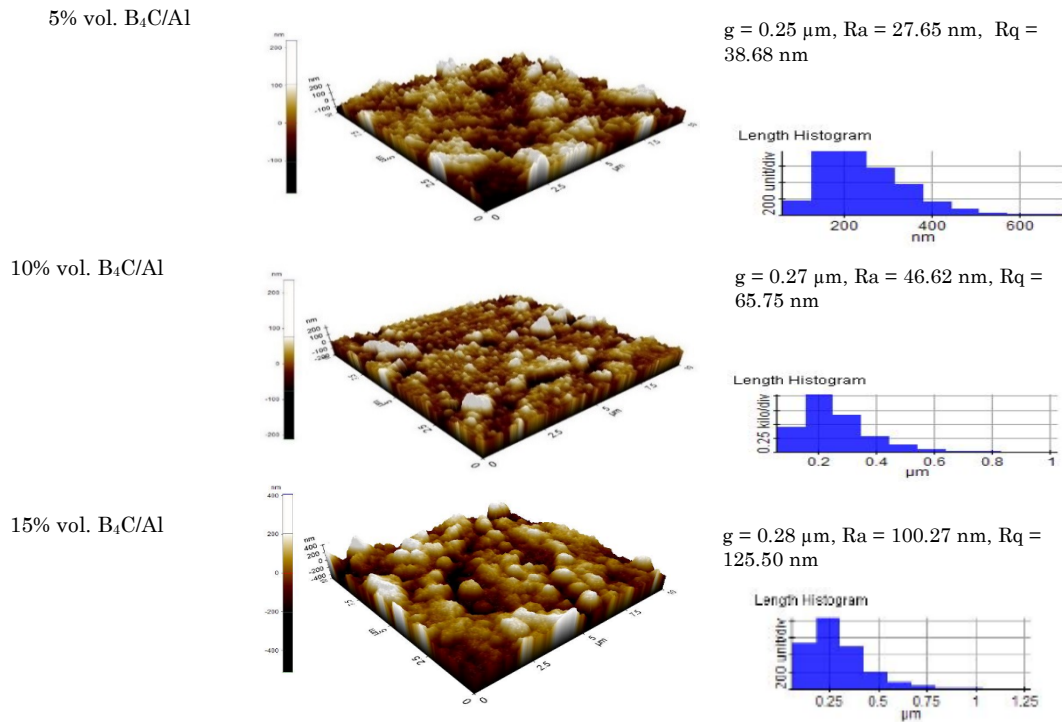$g = 0.28$ μm, Ra = 100.27 nm, Rq = 125.50 nm

Fig 15. AFM topography images of 5% vol. B_4C/Al, 10% vol. B_4C/Al, and 15% vol. B_4C/Al recycled samples under a preheating temperature of 550°C.

3.8. Effect of number of passes on mechanical and microstructure properties

The number of ECAP passes plays a significant role in imposing a high strain rate which is an important influence in the recrystallisation behaviours and improving the mechanical and physical properties of the material. In this research, four number of passes have been proposed to develop a low-cost recycled AA6061-based composite reinforced with B_4C particles. Recycled AA6061 chips mixed with 5% vol. B_4C could be processed up to the 4th pass, and further investigations were carried out for its compressive strength, hardness, density, SEM, EDS, and XRD tests. Despite all of these, there is the enhancement of all presented investigated properties which prove that hot ECAP paves the way of imposing strain, strengthening the boundaries of the material. The mechanical and physical properties of recycled AA6061 reinforced with B_4C on account of the number of passes are shown in Table 7.

3.8.1. Compressive strength test

The compression test was carried out on the recycled MMC samples to investigate the bonds between the AA6061 chips reinforced with B_4C particles by cutting samples to a nominal diameter of 12 and 24 mm in length. The results in Table 7 show that the compressive strength of the MMC increased with the increasing number of passes. The ECAPed materials showed more work hardening and higher compressive strength after the 4th pass (158 MPa) and 3rd pass (152 MPa) than the consolidated samples of 2nd (113 MPa) and 1st (97.9 MPa) passes. The fact is that the consolidated samples contain pores that weaken the recycled MMCs material. The improvement of strength and elastic modulus of the recycled MMC was due to the B_4C, which strengthen the material properties. Also, the matrix produces more dislocations and created pile ups that cause increases in the total material work hardening, which an added reason in the strength of the composites increases (Zhao *et al.* 2005). Moreover, after the 4th pass, the material tends to reach the saturation level and lack independent pressing speed. So, there were no further increases after 5% B_4C and the 4th pass of hot ECAP. Rifai *et al.* (2014) and Selmy *et al.* (2016) confirmed with their observations that the improvement on the MMCs matrix is related to the good bonding between chips and particles during the ECAP process, in which the extensive materials deformations broke up the oxide films on the surface of the sample. Therefore, the material surface ensures better contact bonding between chips. Arab and Akbarzadeh (2013) concluded that further ECAP passes cause more breakage and severe so that, the particles could reach smaller sizes with more braking particles and collision of layers.

3.8.2. Hardness test

Recycled AA6061 chips reinforced with 5% vol. B_4C particles at a different number of passes during the hot ECAP processes. The recycled MMCs after pass four had the highest hardness value, and the overall hardness values gradually increased as a result of increasing the sample's number of passes. The main reason for the material hardness values enhancement was the presence of the total strain and die fraction on the high angle boundaries (Haghighi *et al.* 2012; Selmy *et al.* 2016). The highest value of hardness was achieved for 4th pass, and it is due to the material work hardening, which results in the formation at the initial stage of the hot ECAP process. The hardness increased starting from 53.19, 63.44, 65.23, to 74.95 HV for pass 1, 2, 3, and 4 respectively. However, the decrease in hardness of samples caused the formation of voids and cracks. The imposed strain by the first hot ECAP pass has a superior effect on the breakdown and material refinement of the initial microhardness. Also, the results were increased and it is mainly because of the total exerted strain along with the specimen and die walls during the forming process. As a result of the multiple processes, more MMC samples trapped dislocations and smaller grains were achieved by the hot ECAP forming process and the hardness findings after the fourth pass are about 74.95 HV. Furthermore, an added reason for material test properties enhancement is related to the hard B_4C particles that lead to materials dislocation generation due to the ductility of the 5% vol. B_4C/Al composites. During material dislocations, the interactions with the particles cause leaving loops of residual dislocations surrounded each particle based on the Orowan mechanism (Haghighi *et al.* 2012). The work-hardened strain along the ECAP die surface and billet strengthened the bonds of the MMC, limited the formation of microgrooves on the composites, and decreased the worn MMCs contents. After the 1st pass of ECAP, there were weaker and looser bonds between the particles. However, after the 2nd pass, the material became more robust with fewer voids.

3.8.3. Density test

The density was measured by using the Archimedes method, and distilled water was used for immersing the specimens. The theoretical densities are subjected to the theory of mixture and compared with the measured sample densities. The pores were calculated to find the difference of both measured and theoretical densities (Ramu and Bauri 2009). Table 7 presents the density values of recycled MMC samples, which are 2.628 g/cm^3 (1st pass), 2.64 (2nd pass), 2.65 g/cm^3 (3rd pass), and 2.67 g/cm^3 (4th pass). The bonding between chips and reinforcement particles became denser which means that the multiple passes caused the MMCs to fill the macro voids and cracks more fully resulting in more compact material bonding and higher density. Also, more shear strain by hot ECAP process imposed hydrostatic pressure and improved MMC consolidation. After the 1st pass, the pores were resized to great extents, and more ECAP passes reduced pore number until the 4th pass, which is the saturation point of this investigation. However, extensive nucleation of the voids are predicted and limited to the material enhancement of densities for the density measurement induces that ECAPed recycled samples.

3.8.4. SEM micrographs

Figure 16 shows the SEM results of 5% vol. B_4C/AA6061 recycled samples, processed at 550°C preheating temperature. A good indication in the

interfacial reactions of the processed recycled samples. After the 2nd pass, the residual pores in the recycled samples were eliminated, and the sample's detachment decreased. Furthermore, the amount of plastic work-induced was seen very effectively to minimise the pores of the material on the matrix under multiple ECAP passes with the addition of 5% vol. B_4C. Also, the SEM images of recycled MMC samples from the 1st pass to the 4th pass confirm the extensive material deformation and constant smearing of the processed materials in all directions and fully ultrafine microstructure that demonstrated the chips boundaries as well as the B_4C distributed particles with AA6061 recycled samples.

Moreover, the reinforcements were uniformly distributed in the recycled MMC specimens, and the ECAPed sample's grain boundaries were well defined. The micrographs in Figure 16a,b,c, and d show little porosities and clusters except Figure 16 showed homogeneity of the recycled MMCs samples and hence, agrees with the density results. Forming more oxide layers of the tested MMC sample's surfaces proposed more than two criteria.

Higher plastic strain exerted to break down the oxide layers of the recycled MMCs samples to obtain clean material's contacts. Specific conditions of high processing temperature and pressure to achieve the full complete welding of the B_4C particles and Al chips. When, if the oxides layers are broken, the Al chips are not going for further perfect welding. High pressing compression and shear forces are applied to achieve complete consolidation of the Al/B_4C recycled samples. Derakhshandeh-Haghighi and Jenabali Jahromi (2016) proposed that increasing the number of passes causes extensive material plastic deformation and smearing at all directions. Ramu and

Bauri (2009) confirmed that sample breakage could be observed after multiple times of the ECAP process. Also, Ceschini *et al.* (2009) proposed that representations of shrinkages with material clusters cause incomplete wetting during the solidification process. The density measurement and SEM confirm together with the possibility of reducing voids and defects of the processed materials.

3.8.5. AFM pit morphology

AFM is the standard for microscopy methods used to study and measure surface roughness or test the morphology of micron to nanoparticle shaped thin film surfaces. However, thin films exhibit polycrystalline structure and grain size, which is recommended for thin-film technology investigations. Also, the shape is a factor that influences the grain radius, length, and the like. Therefore, the sharp tip yields higher accuracy (Karoutsos 2014). The results show the possibility of avoiding agglomeration of particles along with the samples. However, the results were altered with multiple time of passes during ECAP forming process. The minimised grains were reported in Table 8 and show the less size from the 1st pass to the 4th pass respectively. So, the decreases of depending on the images surface topography to performed tests (Harichandran and Selvakumar 2015). Attila et al. (Bony n.d.) investigated the effects of process on the materials shape, characteristics, surface structure, and describing responses. In the comparison of all samples with each other, the characterisation of the thermal forming process results on more soft and tin surfaces.
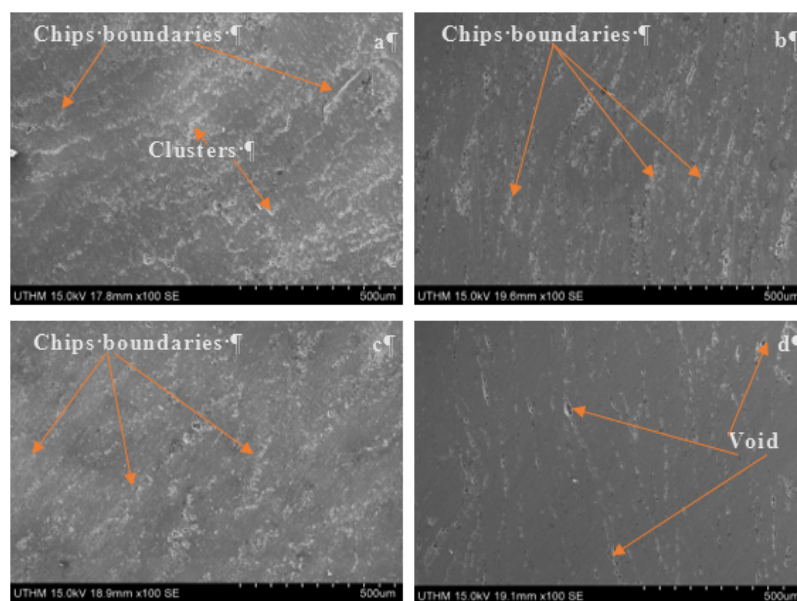

Fig 16. Recycled 5% vol. B4C / AA6061 samples multiple passes (a)1st pass, (b)2nd pass, (c)3rd pass and (d)4th pass

Table 8
AFM mean grain size and surface roughness.

Samples	Mean grain size (µm)	Ra (nm)	Rq (nm)
1st pass	0.26	86.41	82.29
2nd pass	0.25	48.54	61.14
3rd pass	0.23	35.21	56.83
4th pass	0.23	29.43	40.25

1st pass

g = 0.26 µm, Ra = 86.41 nm,

Rq = 82.29 nm

2nd pass

g = 0.25 µm, Ra = 48.54 nm,

Rq = 61.14 nm

3rd pass

g = 0.23 µm, Ra = 35.21 nm,

Rq = 56.83 nm

4th pass
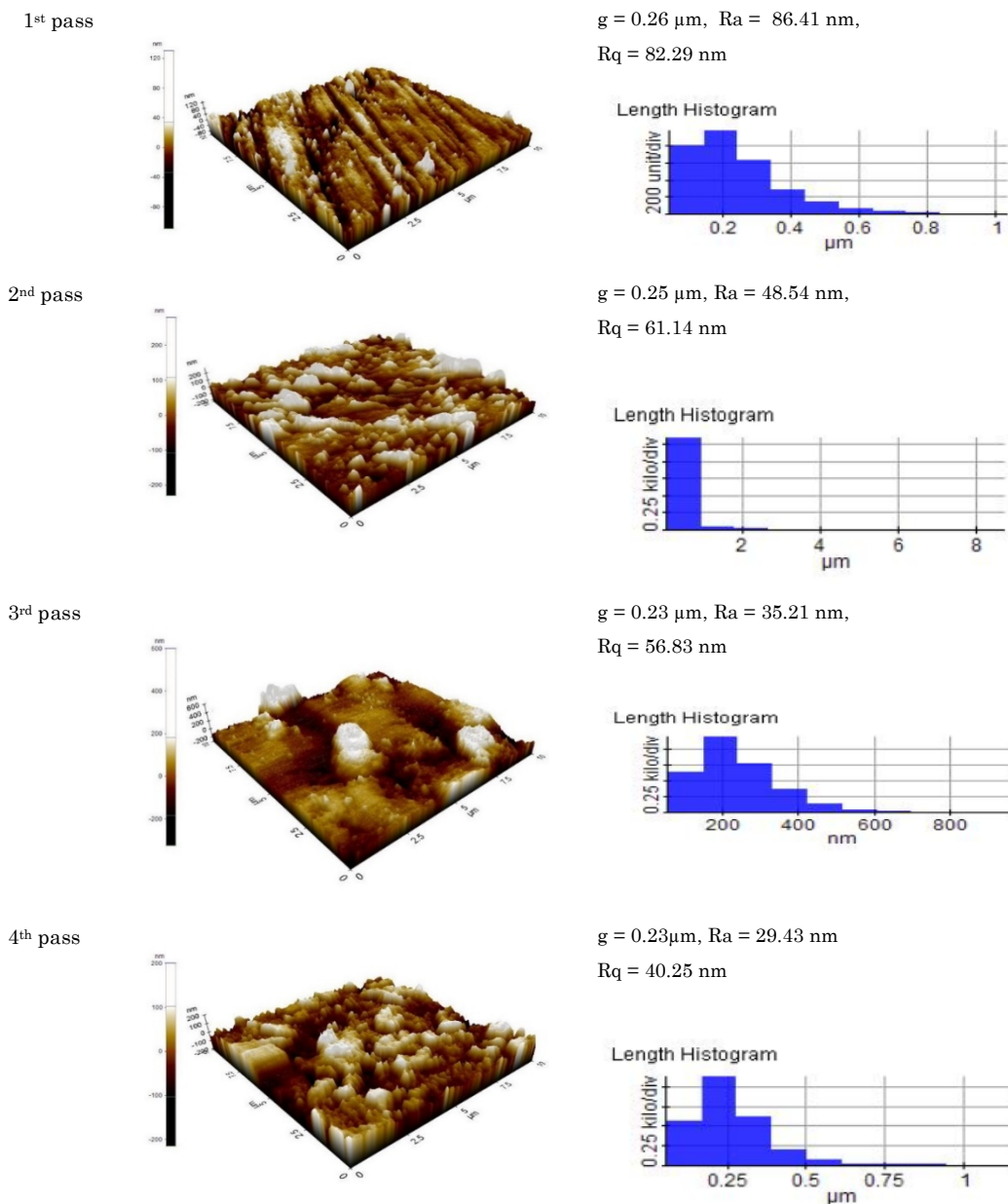
g = 0.23µm, Ra = 29.43 nm

Rq = 40.25 nm

Fig 17. AFM topography images of 5% vol. B_4C/Al after multiple passes.

4. Conclusion

Aluminium chip AA6061-based metal matrix composite reinforced with various volume fractions of B_4C particles was successfully produced by hot ECAP process with introducing Minitab18 software that accomplished the design parameters of recycled $AA6061/B_4C$ composite. The maximum compressive strength and the hardness of the recycled $AA6061/B_4C$ composite were 59.2 MPa and 69 HV, respectively at 5% of B_4C particles and 550°C

processing temperature. Beyond this volumetric percentage, the compressive strength and hardness decreased. Also, XRD investigations show that B_4C is thermodynamically stable and did not produce other compounds where the SEM investigations show minimum pores and well-reinforced particle distributions with 5% vol. B_4C/Al composites. The density and number of pores increased with an increasing volumetric fraction of B_4C beyond 5% of the added B_4C particles. Besides, the volumetric fractions of B_4C and number of passes have a significant effect on the mechanical and physical properties of recycled AA6061/B_4C composite due to that hot ECAP strain hardening and multiple plastic deformation process. Thus, the maximum compressive strength, density and hardness were 158 MPa, 2.67 (g/cm^3) and 74.95 HV were increased, while the grains size, was decreased up to 0.23 μm at the 4th pass of process. Therefore, enhancing the material's mechanical and physical properties by the addition of B_4C particles and developing the ECAP processes as in the case of recycled aluminium chips is more economical and demanding manufacturing process. For future works, investigating the chip size, performing fatigue test reinforced with other sustainable wastes of particles such as natural or industrial ceramics particles could be an added advantages.

Acknowledgment

References

Arab, S.M. and Akbarzadeh, A. (2013) The effect of Equal Channel Angular Pressing process on the microstructure of AZ31 Mg alloy strip shaped specimens. *Journal of Magnesium and Alloys*, 1(2), 145–149.

Bony, A. (2016). AFM characterization of the shape of surface structures with localization factor. *Micron*, 87,1-6

Borblik, V., Korchevoi, A., Nikolenko, A., Strelchuk, V. and Fonkich, A. (2016) Fabrication of Nanostructured Objects by Thermal Vacuum Deposition of Ge Fabrication of Nanostructured Objects by Thermal Vacuum Deposition of Ge Films onto (100) GaAs Substrates. *Nanoscience and Nanoengineering*, 4(1), 22 - 30.

Ceschini, L., Minak, G. and Morri, A. (2009) Forging of the AA2618/20vol.% Al2O3p composite: Effects on microstructure and tensile properties. *Composites Science and Technology*, 69(11–12), 1783–1789.

Derakhshandeh-Haghighi, R. and Jenabali Jahromi, S.A. (2016) The Effect of Multi-pass Equal-Channel Angular Pressing (ECAP) for Consolidation of Aluminum-Nano Alumina Composite Powder on Wear Resistance. *Journal of Materials Engineering and Performance*, 25(2), 687–696.

Djavanroodi, F. and Ebrahimi, M. (2010) Effect of die channel angle, friction and back pressure in the equal channel angular pressing using 3D finite element simulation. *Materials Science and Engineering A*, 527(4–5), 1230–1235.

Fang, D.R., Zhang, Z.F., Wu, S.D., Huang, C.X., Zhang, H., Zhao, N.Q. and Li, J.J. (2006) Effect of equal channel angular pressing on tensile properties and fracture modes of casting Al-Cu alloys. *Materials Science and Engineering A*, 426(1–2), 305–313.

Haghighi, R.D., Jahromi, S.A.J., Moresedgh, A. and Khorshid, M.T. (2012) A comparison between ECAP and conventional extrusion for consolidation of aluminum metal matrix composite. *Journal of Materials Engineering and Performance*, 21(9), 1885–1892.

Harichandran, R. and Selvakumar, N. (2015) ScienceDirect Effect of nano / micro B 4 C particles on the mechanical properties of aluminium metal matrix composites fabricated by ultrasonic cavitation-assisted solidification process. *Archives of Civil and Mechanical Engineering*, 6(1), 1–12. http://dx.doi.org/10.1016/j.acme.2015.07.001.

Karoutsos, V. (2014) Scanning Probe Microscopy : Instrumentation and Applications on Thin Films and Magnetic Multilayers Scanning Probe Microscopy : Instrumentation and Applications on Thin Films and Magnetic Multilayers. *J Nanosci Nanotechnol*, 9(12), 6783-98.

Luce, A. (2007). Atomic Force Microscopy Grain Structure Characterization of Perpendicular Magnetic Recording Media. *2007 REU Research Accomplishment, National Nanotechnology Indratsructure Network*, 134–135.

Qarni, M.J., Sivaswamy, G., Rosochowski, A. and Boczkal, S. (2017) Effect of incremental equal channel angular pressing (I-ECAP) on the microstructural characteristics and mechanical behaviour of commercially pure titanium. *Materials & Design*, 122, 385–402.

Ramu, G. and Bauri, R. (2009) Effect of equal channel angular pressing (ECAP) on microstructure and properties of Al-SiCp composites. *Materials and Design*, 30(9), 3554–3559.

Rebhi, A., Makhlouf, T. and Njah, N. (2009) X-Ray diffraction analysis of 99.1% recycled aluminium subjected to equal channel angular extrusion. *Physics Procedia*, 2(3), 1263–1270.

Rifai, Muhammad, Miyamoto, H., Fujiwara, H. and Rifai, M (2014) The Effect of ECAP Deformation Route on Microstructure, Mechanical and Electrochemical Properties of Low CN Fe-20%Cr Alloy. *Materials Sciences and Applications*, 5(June), 568–578.

Sanusi, K.O., Makinde, O.D. and Oliver, G.J. (2012) Equal channel angular pressing technique for the formation of ultra-fine grained structures. *South African Journal of Science*, 108(9–10), 1–7.

Selmy, A.I., Aal, M.I.A. El and Taha, M.A. (2016) Solid-State Recycling of Aluminum Alloy (AA-6061) Chips via Hot Extrusion Followed by Equal Channel Angular Pressing (ECAP). *The Egyptian International Journal of Engineering Sciences and Technology*, 33–42.

Zhao, N., Nash, P. and Yang, X. (2005) The effect of mechanical alloying on SiC distribution and the properties of 6061 aluminum composite. *Journal of Materials Processing Technology*, 170(3), 586–592.